Chapter 3

LPV Gain-Scheduled Output Feedback for Active Control of Harmonic Disturbances with Time-Varying Frequencies

Pablo Ballesteros, Xinyu Shu, Wiebke Heins and Christian Bohn

Additional information is available at the end of the chapter

http://dx.doi.org/10.5772/50294

1. Introduction

In this chapter, the same control problem as in the previous chapter is considered, which is the rejection of harmonic disturbances with time-varying frequencies for linear time-invariant (LTI) plants. In the previous chapter, gain-scheduled observer-based state-feedback controllers for this control problem were presented. In the present chapter, two methods for the design of general gain-scheduled output-feedback controllers are presented. As in the previous chapter, the control design is based on a description of the system in linear parameter-varying (LPV) form. One of the design methods presented is based on the polytopic linear parameter-varying (pLPV) system description (which has also been used in the previous chapter) and the other method is based on the description of an LPV system in linear fractional transformation (LPV-LFT) form. The basic idea is to use the well-established norm-optimal control framework based on the generalized plant setup shown in Fig. 1 with the generalized plant $\boldsymbol{G}$ and controller $\boldsymbol{K}$.

In this setup, $\boldsymbol{u}$ is the control signal and $\boldsymbol{y}$ consists of all signals that will be provided to the controller. The signal $\boldsymbol{w}$ is the performance input and the signal $\boldsymbol{q}$ is the performance output in the sense that the performance requirements are expressed in terms of the "overall gain" (usually measured by the H_∞ or the H_2 norm) of the transfer function from $\boldsymbol{w}$ to $\boldsymbol{q}$ in closed

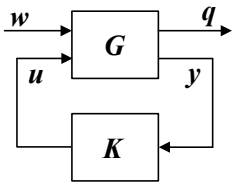

Figure 1. Generalized plant and controller

loop. In this setup, the aim of the controller design is to satisfy performance requirements expressed as upper bounds on the norm (in case of suboptimal control) or minimize the norm (in optimal control) of the transfer function from $\boldsymbol{w}$ to $\boldsymbol{q}$. Loosely speaking, a good controller should make the effect of $\boldsymbol{w}$ on $\boldsymbol{q}$ "small" (for suboptimal control) or "as small as possible" (for optimal control). The performance outputs usually consist of weighted versions of the controlled signal, the control error and the control effort. This is achieved by augmenting the original plant with output weighting functions. Good rejection of specific disturbances can be achieved in this framework by using a disturbance model as a weighting function in the transfer path from the performance input $\boldsymbol{w}$ to the performance output $\boldsymbol{q}$, that is, by modeling the disturbance to be rejected as a weighted version of the performance input. This forces the maximum singular value $\sigma_{\max}(\boldsymbol{G}_{qw}(\mathrm{j}\omega))$ or, in the single-input single-output case, the amplitude response $|G_{qw}(\mathrm{j}\omega)|$ of the open-loop transfer function to have a very high gain in the frequency regions specified by the disturbance model, or, loosely speaking, enlarges the effect of $\boldsymbol{w}$ on $\boldsymbol{q}$ in certain frequency regions. A reduction of the overall effect of $\boldsymbol{w}$ on $\boldsymbol{q}$ in closed loop will then be mostly achieved by reducing the effect in regions where it is large in open loop. From classical control arguments, it is intuitive that this requires a high loop gain in these frequency regions which in turn usually requires a high controller gain. A high loop gain will give a small sensitivity and in turn a good disturbance rejection (in specified frequency regions).

This control design setup is used in this chapter for the rejection of harmonic disturbances with time-varying frequencies. The control design problem is based on a generalized plant obtained through the introduction of a disturbance model that describes the harmonic disturbances and the addition of output weighting functions. Descriptions of the disturbance model in pLPV and in LPV-LFT form are used and lead to generalized plant descriptions that are also in pLPV or LPV-LFT form. Corresponding design methods are then employed to obtain controllers. For a plant in pLPV form, standard H_∞ design [11] is used to compute a set of controllers. The gain scheduling is then achieved by interpolation between these controllers. For a plant in LPV-LFT form, the design method of Apkarian & Gahinet [1] is used that directly yields a gain-scheduled controller also in LPV-LFT form.

LPV approaches for the rejection of harmonic disturbances have been used by Darengosse & Chevrel [7], Du & Shi [8], Du et al. [9], Bohn et al. [5, 6], Kinney & de Callafon [14, 15, 16], Köroğlu & Scherer [17], Witte et al. [19], Balini et al. [4], Heins et al. [12, 13], Ballesteros & Bohn [2, 3] and Shu et al. [18]. Darengosse & Chevrel [7], Du & Shi [8], Du et al. [9], Witte et al. [19], Balini et al. [4] suggested continuous-time LPV approaches. These approaches are tested for a single sinusoidal disturbance by Darengosse & Chevrel [7], Du et al. [9], Witte et al. [19] and Balini et al. [4]. Methods based on observer-based state-feedback controllers are presented by Bohn et al. [5, 6], Kinney & de Callafon [14, 15, 16] and Heins et al. [12, 13]. In the approach of Bohn et al. [5, 6], the observer gain is selected from a set of pre-computed gains by switching. In the other approaches of Kinney & de Callafon [16], Heins et al. [13] and in the previous chapter, the observer gain is calculated by interpolation. In the other approach presented in the previous chapter, which is also used by Kinney & de Callafon [14, 15] and Heins et al. [12], the state-feedback gain is scheduled using interpolation. A general output feedback LPV approach for the rejection of harmonic disturbances is suggested and applied in real time by Ballesteros & Bohn [2, 3] and Shu et al. [18].

The existing LPV approaches can be classified by the control design technique used to obtain the controller. Approaches based on pLPV control design are used by Heins et al. [12, 13],

Kinney & de Callafon [14], Du & Shi [8] and Du et al. [9]. An approach based on LPV-LFT control design is used by Ballesteros & Bohn [2, 3] and Shu et al. [18].

For a practical application, the resulting controller has to be implemented in discrete time. In applications of ANC/AVC, the plant model is often obtained through system identification. This usually gives a discrete-time plant model. If a continuous-time controller is computed, the controller has to be discretized. Since the controller is time varying, this discretization would have to be carried out at each sampling instant. An exact discretization involves the calculation of a matrix exponential, which is computationally too expensive and leads to a distortion of the frequency scale. Usually, this can be tolerated, but not for the suppression of harmonic disturbances. In this context, it is not surprising that the continuous-time design methods of Darengosse & Chevrel [7], Du et al. [9], Kinney & de Callafon [14] and Köroğlu & Scherer [17] are tested only in simulation studies with a very simple system as a plant and a single frequency in the disturbance signal. Exceptions are Witte et al. [19] and Balini et al. [4], who designed continuous-time controllers which then are approximately discretized. However, Witte et al. [19] use a very high sampling frequency of 40 kHz to reject a harmonic disturbance with a frequency up to 48 Hz (in fact, the authors state that they chose "the smallest [sampling time] available by the hardware") and Balini et al. [4] use a maximal sampling frequency of 50 kHz. The control design methods presented in this chapter are realized in discrete time.

The remainder of this chapter is organized as follows. In Sec. 2, pLPV systems and LPV-LFT systems are introduced and the control design for such systems is described. In Sec. 3, it is described how the control problem considered here can be transformed to a generalized plant setup. The required pLPV disturbance model for the harmonic disturbance is introduced in Sec. 3.1 and in Sec. 3.2, it is described how the generalized plant in pLPV form is obtained by combining the disturbance model, the plant and the weighting functions. In Sec. 4, the transformation of the control problem to a generalized plant in LPV-LFT form is treated in essentially the same way, by formulating an LPV-LFT disturbance model (Sec. 4.1) and building a generalized plant in LPV-LFT form (Sec. 4.2). The controller synthesis for both descriptions is described in Sec. 5. Experimental results are presented in Sec. 6 and the chapter finishes with a discussion and some conclusions in Sec. 7.

2. Control design setup

In this section, pLPV systems and LPV-LFT systems are introduced and the control design for such systems is described in Sec. 2.1 and 2.2, respectively.

2.1. Control design for pLPV systems

A pLPV system is of the form

$$\left[\begin{array}{c} \boldsymbol{x}_{k+1} \\ \hline \boldsymbol{y}_k \end{array}\right] = \left[\begin{array}{c|c} \boldsymbol{A}(\boldsymbol{\theta}) & \boldsymbol{B} \\ \hline \boldsymbol{C} & \boldsymbol{D} \end{array}\right] \left[\begin{array}{c} \boldsymbol{x}_k \\ \hline \boldsymbol{u}_k \end{array}\right], \tag{1}$$

where the system matrix depends affinely on a parameter vector $\boldsymbol{\theta}$, that is

$$\boldsymbol{A}(\boldsymbol{\theta}) = \boldsymbol{\mathcal{A}}_0 + \theta_1 \boldsymbol{\mathcal{A}}_1 + \theta_2 \boldsymbol{\mathcal{A}}_2 + \cdots + \theta_N \boldsymbol{\mathcal{A}}_N, \tag{2}$$

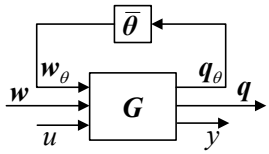

Figure 2. General LPV-LFT system

with constant matrices $\boldsymbol{\mathcal{A}}_i$. The parameter vector $\boldsymbol{\theta}$ varies in a polytope $\boldsymbol{\Theta}$ with M vertices $\boldsymbol{v}_j \in \mathbb{R}^N$. A point $\boldsymbol{\theta} \in \boldsymbol{\Theta}$ can be written as a convex combination of vertices, i.e. there exists a coordinate vector $\boldsymbol{\lambda} = [\,\lambda_1 \cdots \lambda_M\,]^{\mathrm{T}} \in \mathbb{R}^M$ such that $\boldsymbol{\theta}$ can be written as

$$\boldsymbol{\theta} = \sum_{j=1}^{M} \lambda_j \, \boldsymbol{v}_j \tag{3}$$

with

$$\lambda_j \geq 0, \; \sum_{j=1}^{M} \lambda_j = 1. \tag{4}$$

Defining $\boldsymbol{A}_{\mathrm{v},\,j} = \boldsymbol{A}(\boldsymbol{v}_j)$ for $j = 1, \; ..., M$, the system matrix $\boldsymbol{A}(\boldsymbol{\theta})$ can be represented as

$$\boldsymbol{A}(\boldsymbol{\theta}) = \boldsymbol{A}(\boldsymbol{\lambda}) = \lambda_1 \boldsymbol{A}_{\mathrm{v},\,1} + \lambda_2 \boldsymbol{A}_{\mathrm{v},\,2} + ... + \lambda_M \boldsymbol{A}_{\mathrm{v},\,M}. \tag{5}$$

The system matrix of a pLPV system $\boldsymbol{A}(\boldsymbol{\theta})$ can be calculated from the M vertices of the polytope $\boldsymbol{\Theta}$ by finding the coordinate vector $\boldsymbol{\lambda}$ that fulfills the conditions of (3) and (4).

Once a representation of a system is obtained in pLPV form, it is possible to find a controller using H_∞ or H_2 techniques for each vertex of the polytope. The controller for a given $\boldsymbol{\theta} \in \boldsymbol{\Theta}$ can be calculated through controllers for the vertex systems. The closed-loop stability is guaranteed even for arbitrarily fast changes of the scheduling parameters if a parameter-independent Lyapunov function is used (for the whole polytope) in the control design. This approach, however, is conservative because fast variations of the scheduling parameters are considered, which might not occur in a practical application. Parameter-dependent Lyapunov functions can be used to include bounds on the rate of change of the parameters, but are not considered here.

2.2. Control design for LPV-LFT systems

An LPV system in LFT form is shown in Fig. 2. It consists of a generalized plant $\boldsymbol{G}$ that includes input and output weighting functions and a parametric uncertainty block $\bar{\boldsymbol{\theta}}$ that has been "pulled out" of the system. For this general system, a gain-scheduling controller can be calculated following the method presented in Apkarian & Gahinet [1]. In this method, two sets of linear matrix inequalities (LMIs) are solved. The first set of LMIs determines the feasibility of the problem which means that a bound on the control system performance in the sense of the H_∞ norm can be satisfied. With the second set of LMIs, the controller matrices are calculated from the solution of the first set of LMIs.

As a result of applying this control design method, the gain-scheduling control structure of Fig. 3 is obtained. The time-varying plant parameters are directly used as the gain-scheduling

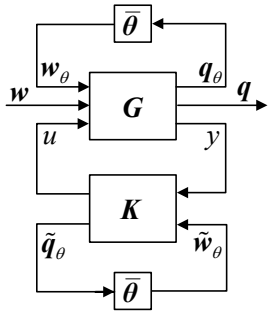

Figure 3. LPV-LFT gain-scheduling control structure

parameters of the controller. This control design method guarantees stability through the small gain theorem. It is often conservative, since the parameter ranges covered are usually larger than the ones that may occur in the real system.

3. Generalized plant in pLPV form

As stated in the previous section, to calculate the controller using the pLPV control design method, the generalized plant in pLPV form is needed. In this section, the steps to obtain the generalized plant in pLPV form are discussed. The disturbance model and a representation of the disturbance model in pLPV form are obtained in Sec. 3.1. In Sec. 3.2, the generalized plant is built by combining the plant, the disturbance model in pLPV form and the weighting functions.

3.1. Disturbance model

A general model for a harmonic disturbance with n_d fixed frequencies is described by

$$\left[\begin{array}{c|c} \boldsymbol{A}_\mathrm{d} & \boldsymbol{B}_\mathrm{d} \\ \hline \boldsymbol{C}_\mathrm{d} & 0 \end{array}\right] \tag{6}$$

with

$$\boldsymbol{A}_\mathrm{d} = \begin{bmatrix} \boldsymbol{A}_{\mathrm{d},1} & \cdots & \boldsymbol{0} \\ \vdots & \ddots & \vdots \\ \boldsymbol{0} & \cdots & \boldsymbol{A}_{\mathrm{d},n_\mathrm{d}} \end{bmatrix}, \ \boldsymbol{A}_{\mathrm{d},i} = \begin{bmatrix} 0 & 1 \\ -1 & a_i \end{bmatrix}, \tag{7}$$

$$a_i = 2\cos(2\pi f_i T), \tag{8}$$

$$\boldsymbol{B}_\mathrm{d} = \begin{bmatrix} \boldsymbol{B}_{\mathrm{d},1} \\ \vdots \\ \boldsymbol{B}_{\mathrm{d},n_\mathrm{d}} \end{bmatrix}, \ \boldsymbol{B}_{\mathrm{d},i} = \begin{bmatrix} 1 \\ 1 \end{bmatrix}, \tag{9}$$

$$\boldsymbol{C}_\mathrm{d} = \begin{bmatrix} \boldsymbol{C}_{\mathrm{d},1} & \cdots & \boldsymbol{C}_{\mathrm{d},n_\mathrm{d}} \end{bmatrix} \text{ and } \boldsymbol{C}_{\mathrm{d},i} = \begin{bmatrix} 1 & 0 \end{bmatrix}. \tag{10}$$

A harmonic disturbance can be modeled as the output of an unforced system with system matrix $\boldsymbol{A}_\mathrm{d}$ and output matrix $\boldsymbol{C}_\mathrm{d}$ given above in (7) and (10). An input matrix is not

required. However, in the generalized plant setup, a performance input is required and the disturbance model acts as an input weighting function on the performance input. This is why the disturbance model above has been given with a nonzero input matrix $\boldsymbol{B}_\mathrm{d}$ in (9).

The frequency in (8) is fixed and denoted by f_i. As in Sec. 4 of the previous chapter, the pLPV disturbance model for n_d time-varying frequencies $f_{j,k} \in [f_{\min,j}, f_{\max,j}]$, $j = 1, 2, \ldots, n_\mathrm{d}$, is defined as

$$\left[\begin{array}{c|c} \boldsymbol{A}_\mathrm{d}^{(\mathrm{pLPV})}(\boldsymbol{\theta}) & \boldsymbol{B}_\mathrm{d}^{(\mathrm{pLPV})} \\ \hline \boldsymbol{C}_\mathrm{d}^{(\mathrm{pLPV})} & 0 \end{array}\right] \tag{11}$$

with

$$\boldsymbol{A}_\mathrm{d}^{(\mathrm{pLPV})}(\boldsymbol{\theta}) = \boldsymbol{\mathcal{A}}_{\mathrm{d},\,0} + \theta_1 \boldsymbol{\mathcal{A}}_{\mathrm{d},\,1} + \cdots + \theta_{n_\mathrm{d}}\, \boldsymbol{\mathcal{A}}_{\mathrm{d},\,n_\mathrm{d}}. \tag{12}$$

As in Sec. 2.1, (12) can be written in the form of

$$\boldsymbol{A}_\mathrm{d}^{(\mathrm{pLPV})}(\boldsymbol{\theta}) = \boldsymbol{A}_\mathrm{d}^{(\mathrm{pLPV})}(\boldsymbol{\lambda}) = \lambda_1 \boldsymbol{A}_{\mathrm{v},\,1} + \cdots + \lambda_M \boldsymbol{A}_{\mathrm{v},\,M} = \sum_{i=1}^{M} \lambda_i \boldsymbol{A}_{\mathrm{v},\,i}, \tag{13}$$

where the matrices $\boldsymbol{A}_{\mathrm{v},\,i}$ are defined in the same way as $\boldsymbol{A}_\mathrm{d}^{(\mathrm{pLPV})}$ in (7) and (8), but with a_i evaluated for all the vertices of the polytope, with $j = 1, 2, \ldots, n_\mathrm{d}$. The coordinate vector $\boldsymbol{\lambda}$ can be calculated using the method described in Sec. 4.4 of the previous chapter.

3.2. Generalized plant

A state-space representation of the plant is given by

$$G_\mathrm{p} = \left[\begin{array}{c|c} \boldsymbol{A}_\mathrm{p} & \boldsymbol{B}_\mathrm{p} \\ \hline \boldsymbol{C}_\mathrm{p} & D_\mathrm{p} \end{array}\right] \tag{14}$$

and it is assumed that the disturbance is acting on the input of the plant.

The block diagram of the generalized plant with the disturbance, the plant and the weighting functions

$$W_y^{(\mathrm{pLPV})} = \left[\begin{array}{c|c} \boldsymbol{A}_{W_y}^{(\mathrm{pLPV})} & \boldsymbol{B}_{W_y}^{(\mathrm{pLPV})} \\ \hline \boldsymbol{C}_{W_y}^{(\mathrm{pLPV})} & D_{W_y}^{(\mathrm{pLPV})} \end{array}\right], \tag{15}$$

$$W_u^{(\mathrm{pLPV})} = \left[\begin{array}{c|c} \boldsymbol{A}_{W_u}^{(\mathrm{pLPV})} & \boldsymbol{B}_{W_u}^{(\mathrm{pLPV})} \\ \hline \boldsymbol{C}_{W_u}^{(\mathrm{pLPV})} & D_{W_u}^{(\mathrm{pLPV})} \end{array}\right] \tag{16}$$

is illustrated in Fig. 4.

For every vertex of the polytopic system, the generalized plant can be described by

$$\begin{bmatrix} \boldsymbol{x}_{k+1} \\ \boldsymbol{q}_k \\ y_k \end{bmatrix} = \left[\begin{array}{c|cc} \boldsymbol{A}_i(\boldsymbol{\theta}) & \boldsymbol{B}_w^{(\mathrm{pLPV})} & \boldsymbol{B}_u^{(\mathrm{pLPV})} \\ \hline \boldsymbol{C}_q^{(\mathrm{pLPV})} & \boldsymbol{D}_{qw}^{(\mathrm{pLPV})} & \boldsymbol{D}_{qu}^{(\mathrm{pLPV})} \\ \boldsymbol{C}_y^{(\mathrm{pLPV})} & D_{yw}^{(\mathrm{pLPV})} & D_{yu}^{(\mathrm{pLPV})} \end{array}\right] \begin{bmatrix} \boldsymbol{x}_k \\ w_k \\ u_k \end{bmatrix} \tag{17}$$

where

$$\boldsymbol{x}_k = \left[\boldsymbol{x}_{\mathrm{p},k}^\mathrm{T}\ \boldsymbol{x}_{\mathrm{d},k}^\mathrm{T}\ \boldsymbol{x}_{W_y,k}^\mathrm{T}\ \boldsymbol{x}_{W_u,k}^\mathrm{T}\right]^\mathrm{T}, \tag{18}$$

$$\boldsymbol{A}_i(\boldsymbol{\theta}) = \begin{bmatrix} \boldsymbol{A}_\mathrm{p} & \boldsymbol{B}_\mathrm{p}\boldsymbol{C}_\mathrm{d}^{(\mathrm{pLPV})} & \boldsymbol{0} & \boldsymbol{0} \\ \boldsymbol{0} & \boldsymbol{A}_{\mathrm{v},i} & \boldsymbol{0} & \boldsymbol{0} \\ \boldsymbol{B}_{W_y}^{(\mathrm{pLPV})}\boldsymbol{C}_\mathrm{p} & \boldsymbol{0} & \boldsymbol{A}_{W_y}^{(\mathrm{pLPV})} & \boldsymbol{0} \\ \boldsymbol{0} & \boldsymbol{0} & \boldsymbol{0} & \boldsymbol{A}_{W_u}^{(\mathrm{pLPV})} \end{bmatrix}, \tag{19}$$

$$\begin{bmatrix} \boldsymbol{B}_w^{(\mathrm{pLPV})} & \boldsymbol{B}_u^{(\mathrm{pLPV})} \end{bmatrix} = \begin{bmatrix} \boldsymbol{0} & \boldsymbol{B}_\mathrm{p} \\ \boldsymbol{B}_\mathrm{d}^{(\mathrm{pLPV})} & \boldsymbol{0} \\ \boldsymbol{0} & \boldsymbol{0} \\ \boldsymbol{0} & \boldsymbol{B}_{W_u}^{(\mathrm{pLPV})} \end{bmatrix}, \tag{20}$$

$$\begin{bmatrix} \boldsymbol{C}_q^{(\mathrm{pLPV})} \\ \boldsymbol{C}_y^{(\mathrm{pLPV})} \end{bmatrix} = \left[\begin{array}{cccc} D_{W_y}^{(\mathrm{pLPV})}\boldsymbol{C}_\mathrm{p} & \boldsymbol{0} & \boldsymbol{C}_{W_y}^{(\mathrm{pLPV})} & \boldsymbol{0} \\ \boldsymbol{0} & \boldsymbol{0} & \boldsymbol{0} & \boldsymbol{C}_{W_u}^{(\mathrm{pLPV})} \\ \hline \boldsymbol{C}_\mathrm{p} & \boldsymbol{0} & \boldsymbol{0} & \boldsymbol{0} \end{array}\right] \tag{21}$$

and

$$\begin{bmatrix} \boldsymbol{D}_{qw}^{(\mathrm{pLPV})} & \boldsymbol{D}_{qu}^{(\mathrm{pLPV})} \\ D_{yw}^{(\mathrm{pLPV})} & D_{yu}^{(\mathrm{pLPV})} \end{bmatrix} = \left[\begin{array}{cc} 0 & 0 \\ 0 & D_{W_u}^{(\mathrm{pLPV})} \\ \hline 0 & 0 \end{array}\right]. \tag{22}$$

Once the generalized plant is obtained, the controller can be calculated using the algorithms in the following section.

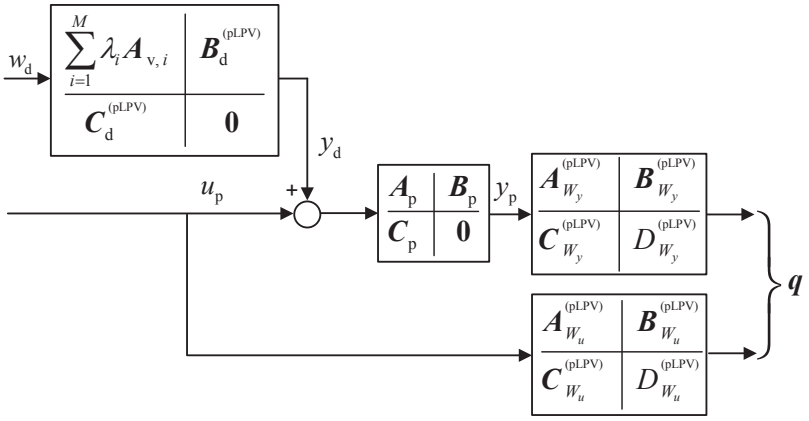

Figure 4. Plant with pLPV disturbance model and weighting functions

4. Generalized plant in LPV-LFT form

The same steps as in the previous section are carried out, but in this section the generalized plant in LPV-LFT form is obtained such that the control design method of Apkarian & Gahinet [1] can be used. The model of the harmonic disturbance and the generalized plant in LFT form are obtained in Sec. 4.1 and 4.2, respectively. The generalized plant is the result of combining plant, harmonic disturbance and weighting functions.

4.1. Disturbance model

The state-space representation of a harmonic disturbance for n_d fixed frequencies was given by (6-10). If the frequencies of a harmonic disturbance change between minimal values $f_{i,\min}$ and maximal values $f_{i,\max}$, a representation for the variations of the frequencies is given by

$$a_i(f_i) = 2\cos(2\pi f_i T) = \overline{a}_i + p_i \overline{\theta}_{i,k}(f_i) \tag{23}$$

with

$$\overline{a}_i = \cos(2\pi f_{i,\max} T) + \cos(2\pi f_{i,\min} T), \tag{24}$$

$$p_i = \cos(2\pi f_{i,\max} T) - \cos(2\pi f_{i,\min} T) \tag{25}$$

and

$$\overline{\theta}_{i,k} \in [-1,\, 1]. \tag{26}$$

An LPV-LFT model of the disturbance can be written as

$$\boldsymbol{x}_{\mathrm{d},k+1} = \boldsymbol{A}_\mathrm{d}\boldsymbol{x}_{\mathrm{d},k} + \boldsymbol{B}_{\mathrm{d},\theta}\boldsymbol{w}_{\theta,k} + \boldsymbol{B}_{\mathrm{d},w} w_{\mathrm{d},k}, \tag{27}$$

$$\boldsymbol{q}_{\theta,k} = \boldsymbol{C}_{\mathrm{d},\theta}\boldsymbol{x}_{\mathrm{d},k}, \tag{28}$$

$$y_{\mathrm{d},k} = \boldsymbol{C}_{\mathrm{d},y}\boldsymbol{x}_{\mathrm{d},k}, \tag{29}$$

$$\boldsymbol{w}_{\theta,k} = \overline{\boldsymbol{\theta}}_k \boldsymbol{q}_{\theta,k} \tag{30}$$

with

$$\boldsymbol{A}_\mathrm{d} = \begin{bmatrix} \boldsymbol{A}_{\mathrm{d},1} & \cdots & \boldsymbol{0} \\ \vdots & \ddots & \vdots \\ \boldsymbol{0} & \cdots & \boldsymbol{A}_{\mathrm{d},n_\mathrm{d}} \end{bmatrix},\ \boldsymbol{A}_{\mathrm{d},i} = \begin{bmatrix} 0 & 1 \\ -1 & \overline{a}_i \end{bmatrix}, \tag{31}$$

$$\boldsymbol{B}_{\mathrm{d},\theta} = \begin{bmatrix} \boldsymbol{B}_{\mathrm{d},\theta,1} & \cdots & \boldsymbol{0} \\ \vdots & \ddots & \vdots \\ \boldsymbol{0} & \cdots & \boldsymbol{B}_{\mathrm{d},\theta,n_\mathrm{d}} \end{bmatrix},\ \boldsymbol{B}_{\mathrm{d},\theta,i} = \begin{bmatrix} 0 \\ p_i \end{bmatrix}, \tag{32}$$

$$\boldsymbol{B}_{\mathrm{d},w} = \begin{bmatrix} \boldsymbol{B}_{\mathrm{d},w,1} \\ \vdots \\ \boldsymbol{B}_{\mathrm{d},w,n_\mathrm{d}} \end{bmatrix},\ \boldsymbol{B}_{\mathrm{d},w,i} = \begin{bmatrix} 1 \\ 1 \end{bmatrix}, \tag{33}$$

$$\boldsymbol{C}_{\mathrm{d},\theta} = \begin{bmatrix} \boldsymbol{C}_{\mathrm{d},\theta,1} & \cdots & \boldsymbol{0} \\ \vdots & \ddots & \vdots \\ \boldsymbol{0} & \cdots & \boldsymbol{C}_{\mathrm{d},\theta,n_\mathrm{d}} \end{bmatrix},\ \boldsymbol{C}_{\mathrm{d},\theta,i} = \begin{bmatrix} 0 & 1 \end{bmatrix}, \tag{34}$$

$$\boldsymbol{C}_{\mathrm{d},y} = \begin{bmatrix} \boldsymbol{C}_{\mathrm{d},y,1} & \cdots & \boldsymbol{C}_{\mathrm{d},y,n_\mathrm{d}} \end{bmatrix},\ \boldsymbol{C}_{\mathrm{d},y,i} = \begin{bmatrix} 1 & 0 \end{bmatrix} \tag{35}$$

and

$$\overline{\boldsymbol{\theta}}_k = \begin{bmatrix} \overline{\theta}_{1,k} & \cdots & 0 \\ \vdots & \ddots & \vdots \\ 0 & \cdots & \overline{\theta}_{n_\mathrm{d},k} \end{bmatrix}. \tag{36}$$

4.2. Generalized plant

The generalized plant is the result of combining the plant, the harmonic disturbance and the weighting functions and it is shown in Fig. 5. The weighting functions are defined the same way as in (15) and (16). A representation of the generalized plant in LFT form is given by

$$\begin{bmatrix} \boldsymbol{x}_{k+1} \\ \boldsymbol{q}_{\theta,k} \\ \boldsymbol{q}_k \\ y_k \end{bmatrix} = \left[\begin{array}{c|ccc} \boldsymbol{A} & \boldsymbol{B}_\theta & \boldsymbol{B}_w^{(\mathrm{LFT})} & \boldsymbol{B}_u^{(\mathrm{LFT})} \\ \hline \boldsymbol{C}_\theta & \boldsymbol{D}_{\theta\theta} & \boldsymbol{D}_{\theta w} & \boldsymbol{D}_{\theta u} \\ \boldsymbol{C}_q^{(\mathrm{LFT})} & \boldsymbol{D}_{q\theta} & \boldsymbol{D}_{qw}^{(\mathrm{LFT})} & \boldsymbol{D}_{qu}^{(\mathrm{LFT})} \\ \boldsymbol{C}_y^{(\mathrm{LFT})} & \boldsymbol{D}_{y\theta} & \boldsymbol{D}_{yw}^{(\mathrm{LFT})} & \boldsymbol{D}_{yu}^{(\mathrm{LFT})} \end{array}\right] \begin{bmatrix} \boldsymbol{x}_k \\ \boldsymbol{w}_{\theta,k} \\ \boldsymbol{w}_k \\ u_k \end{bmatrix} \tag{37}$$

with

$$\boldsymbol{x}_k = \begin{bmatrix} \boldsymbol{x}_{\mathrm{p},k}^{\mathrm{T}} & \boldsymbol{x}_{\mathrm{d},k}^{\mathrm{T}} & \boldsymbol{x}_{W_y,k}^{\mathrm{T}} & \boldsymbol{x}_{W_u,k}^{\mathrm{T}} \end{bmatrix}^{\mathrm{T}}, \tag{38}$$

$$\boldsymbol{A} = \begin{bmatrix} \boldsymbol{A}_\mathrm{p} & \boldsymbol{B}_\mathrm{p}\boldsymbol{C}_{\mathrm{d},y} & \boldsymbol{0} & \boldsymbol{0} \\ \boldsymbol{0} & \boldsymbol{A}_\mathrm{d} & \boldsymbol{0} & \boldsymbol{0} \\ \boldsymbol{B}_{W_y}^{(\mathrm{LFT})}\boldsymbol{C}_\mathrm{p} & \boldsymbol{0} & \boldsymbol{A}_{W_y}^{(\mathrm{LFT})} & \boldsymbol{0} \\ \boldsymbol{0} & \boldsymbol{0} & \boldsymbol{0} & \boldsymbol{A}_{W_u}^{(\mathrm{LFT})} \end{bmatrix}, \tag{39}$$

$$\begin{bmatrix} \boldsymbol{B}_\theta & \boldsymbol{B}_w^{(\mathrm{LFT})} & \boldsymbol{B}_u^{(\mathrm{LFT})} \end{bmatrix} = \begin{bmatrix} \boldsymbol{0} & \boldsymbol{0} & \boldsymbol{B}_\mathrm{p} \\ \boldsymbol{B}_{\mathrm{d},\theta} & \boldsymbol{B}_{\mathrm{d},w} & \boldsymbol{0} \\ \boldsymbol{0} & \boldsymbol{0} & \boldsymbol{0} \\ \boldsymbol{0} & \boldsymbol{0} & \boldsymbol{B}_{W_u}^{(\mathrm{LFT})} \end{bmatrix}, \tag{40}$$

$$\begin{bmatrix} \boldsymbol{C}_\theta \\ \boldsymbol{C}_q^{(\mathrm{LFT})} \\ \boldsymbol{C}_y^{(\mathrm{LFT})} \end{bmatrix} = \left[\begin{array}{cccc} \boldsymbol{0} & \boldsymbol{C}_{\mathrm{d},\theta} & \boldsymbol{0} & \boldsymbol{0} \\ \hline \boldsymbol{D}_{W_y}^{(\mathrm{LFT})}\boldsymbol{C}_\mathrm{p} & \boldsymbol{0} & \boldsymbol{C}_{W_y}^{(\mathrm{LFT})} & \boldsymbol{0} \\ \boldsymbol{0} & \boldsymbol{0} & \boldsymbol{0} & \boldsymbol{C}_{W_u}^{(\mathrm{LFT})} \\ \hline \boldsymbol{C}_\mathrm{p} & \boldsymbol{0} & \boldsymbol{0} & \boldsymbol{0} \end{array}\right] \tag{41}$$

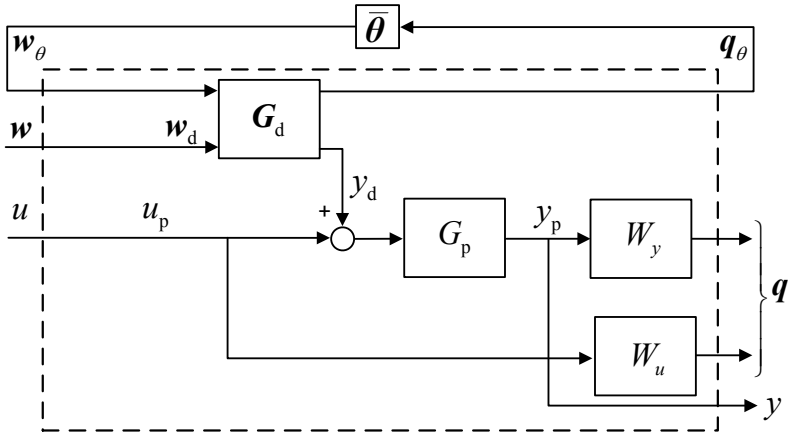

Figure 5. Plant with LPV-LFT disturbance model and weighting functions

and

$$\begin{bmatrix} \boldsymbol{D}_{\theta\theta} & \boldsymbol{D}_{\theta w} & \boldsymbol{D}_{\theta u} \\ \boldsymbol{D}_{q\theta} & \boldsymbol{D}_{qw}^{(\mathrm{LFT})} & \boldsymbol{D}_{qu}^{(\mathrm{LFT})} \\ \boldsymbol{D}_{y\theta} & D_{yw}^{(\mathrm{LFT})} & D_{yu}^{(\mathrm{LFT})} \end{bmatrix} = \left[\begin{array}{cc|c} \boldsymbol{0} & \boldsymbol{0} & \boldsymbol{0} \\ \hline \boldsymbol{0} & 0 & 0 \\ \boldsymbol{0} & 0 & D_{W_u}^{(\mathrm{LFT})} \\ \hline \boldsymbol{0} & 0 & 0 \end{array}\right]. \tag{42}$$

5. Controller synthesis and implementation for LPV systems

In this section, algorithms for the calculation of the pLPV and LPV-LFT gain-scheduling controllers are explained in detail. Suboptimal controllers using H_∞ techniques are obtained.

5.1. Controller synthesis and implementation for pLPV systems

With the generalized plant in pLPV form, an H_∞-suboptimal controller for each vertex of the polytope can be calculated using standard H_∞ techniques [11]. The steps to obtain them are explained here in detail.

First, two outer factors

$$\boldsymbol{N}_{\boldsymbol{X}} = \mathrm{null}\left[\boldsymbol{C}_y^{(\mathrm{pLPV})} \;\; \boldsymbol{D}_{yw}^{(\mathrm{pLPV})} \;\; \boldsymbol{0}\right] \tag{43}$$

and

$$\boldsymbol{N}_{\boldsymbol{Y}} = \mathrm{null}\left[(\boldsymbol{B}_u^{(\mathrm{pLPV})})^{\mathrm{T}} \;\; (\boldsymbol{D}_{qu}^{(\mathrm{pLPV})})^{\mathrm{T}} \;\; 0\right] \tag{44}$$

are defined, where null$[\cdot]$ denotes the basis of the null space of a matrix.

Then, the LMIs

$$\boldsymbol{N}_{\boldsymbol{X}}^{\mathrm{T}} \begin{bmatrix} \boldsymbol{A}_i^{\mathrm{T}}\boldsymbol{X}_1\boldsymbol{A}_i - \boldsymbol{X}_1 & \boldsymbol{A}_i^{\mathrm{T}}\boldsymbol{X}_1\boldsymbol{B}_w^{(\mathrm{pLPV})} & (\boldsymbol{C}_q^{(\mathrm{pLPV})})^{\mathrm{T}} \\ (\boldsymbol{B}_w^{(\mathrm{pLPV})})^{\mathrm{T}}\boldsymbol{X}_1\boldsymbol{A}_i & -\gamma + (\boldsymbol{B}_w^{(\mathrm{pLPV})})^{\mathrm{T}}\boldsymbol{X}_1\boldsymbol{B}_w^{(\mathrm{pLPV})} & (\boldsymbol{D}_{qu}^{(\mathrm{pLPV})})^{\mathrm{T}} \\ \boldsymbol{C}_q^{(\mathrm{pLPV})} & \boldsymbol{D}_{qu}^{(\mathrm{pLPV})} & -\gamma\mathbf{I} \end{bmatrix} \boldsymbol{N}_{\boldsymbol{X}} < 0, \tag{45}$$

$$\boldsymbol{N}_{\boldsymbol{Y}}^{\mathrm{T}} \begin{bmatrix} \boldsymbol{A}_i\boldsymbol{Y}_1\boldsymbol{A}_i^{\mathrm{T}} - \boldsymbol{Y}_1 & \boldsymbol{A}_i\boldsymbol{Y}_1(\boldsymbol{C}_q^{(\mathrm{pLPV})})^{\mathrm{T}} & \boldsymbol{B}_w^{(\mathrm{pLPV})} \\ \boldsymbol{C}_q^{(\mathrm{pLPV})}\boldsymbol{Y}_1\boldsymbol{A}_i^{\mathrm{T}} & -\gamma\mathbf{I} + \boldsymbol{C}_q^{(\mathrm{pLPV})}\boldsymbol{Y}_1(\boldsymbol{C}_q^{(\mathrm{pLPV})})^{\mathrm{T}} & \boldsymbol{D}_{qu}^{(\mathrm{pLPV})} \\ (\boldsymbol{B}_w^{(\mathrm{pLPV})})^{\mathrm{T}} & (\boldsymbol{D}_{qu}^{(\mathrm{pLPV})})^{\mathrm{T}} & -\gamma \end{bmatrix} \boldsymbol{N}_{\boldsymbol{Y}} < 0, \tag{46}$$

$$\begin{bmatrix} \boldsymbol{X}_1 & \mathbf{I} \\ \mathbf{I} & \boldsymbol{Y}_1 \end{bmatrix} \geq 0 \tag{47}$$

for feasibility and optimality are solved for $\boldsymbol{X}_1$ and $\boldsymbol{Y}_1$ for every $\boldsymbol{A}_i = \boldsymbol{A}_i(\boldsymbol{\theta})$.

With $\boldsymbol{X}_1$ and $\boldsymbol{Y}_1$, the matrices

$$\boldsymbol{X}_1 - \boldsymbol{Y}_1^{-1} = \boldsymbol{X}_2^{\mathrm{T}}\boldsymbol{X}_2, \tag{48}$$

$$\boldsymbol{X}^{(\mathrm{pLPV})} = \begin{bmatrix} \boldsymbol{X}_1 & \boldsymbol{X}_2 \\ \boldsymbol{X}_2^{\mathrm{T}} & \mathbf{I} \end{bmatrix} \tag{49}$$

are calculated.

With

$$\overline{\boldsymbol{A}}_i = \begin{bmatrix} \boldsymbol{A}_i & \boldsymbol{0} \\ \boldsymbol{0} & \boldsymbol{0} \end{bmatrix}, \tag{50}$$

$$\overline{\boldsymbol{B}} = \begin{bmatrix} \boldsymbol{B}_w^{(\mathrm{pLPV})} \\ \mathbf{0} \end{bmatrix}, \tag{51}$$

$$\overline{\boldsymbol{C}} = \begin{bmatrix} \boldsymbol{C}_q^{(\mathrm{pLPV})} & \mathbf{0} \end{bmatrix}, \tag{52}$$

the matrix

$$\boldsymbol{\psi}_i = \begin{bmatrix} -(\boldsymbol{X}^{(\mathrm{pLPV})})^{-1} & \overline{\boldsymbol{A}}_i & \overline{\boldsymbol{B}} & \mathbf{0} \\ \overline{\boldsymbol{A}}_i^{\mathrm{T}} & -\boldsymbol{X}^{(\mathrm{pLPV})} & \mathbf{0} & \overline{\boldsymbol{C}}^{\mathrm{T}} \\ \overline{\boldsymbol{B}}^{\mathrm{T}} & \mathbf{0} & -\gamma & (\boldsymbol{D}_{qw}^{(\mathrm{pLPV})})^{\mathrm{T}} \\ \mathbf{0} & \overline{\boldsymbol{C}} & \boldsymbol{D}_{qw}^{(\mathrm{pLPV})} & -\gamma\mathbf{I} \end{bmatrix}. \tag{53}$$

is calculated. The matrices

$$\boldsymbol{P}^{(\mathrm{pLPV})} = \begin{bmatrix} \underline{\boldsymbol{B}}^{\mathrm{T}} & \mathbf{0} & \mathbf{0} & \underline{\boldsymbol{D}}_{qu}^{\mathrm{T}} \end{bmatrix} \tag{54}$$

and

$$\boldsymbol{Q}^{(\mathrm{pLPV})} = \begin{bmatrix} \mathbf{0} & \underline{\boldsymbol{C}} & \underline{\boldsymbol{D}}_{yw} & \mathbf{0} \end{bmatrix} \tag{55}$$

are composed with

$$\underline{\boldsymbol{B}} = \begin{bmatrix} \mathbf{0} & \boldsymbol{B}_u^{(\mathrm{pLPV})} \\ \mathbf{I} & \mathbf{0} \end{bmatrix}, \tag{56}$$

$$\underline{\boldsymbol{C}} = \begin{bmatrix} \mathbf{0} & \mathbf{I} \\ \boldsymbol{C}_y^{(\mathrm{pLPV})} & \mathbf{0} \end{bmatrix}, \tag{57}$$

$$\underline{\boldsymbol{D}}_{qu} = \begin{bmatrix} \mathbf{0} & \boldsymbol{D}_{qu}^{(\mathrm{pLPV})} \end{bmatrix}, \tag{58}$$

$$\underline{\boldsymbol{D}}_{yw} = \begin{bmatrix} \mathbf{0} \\ D_{yw}^{(\mathrm{pLPV})} \end{bmatrix}. \tag{59}$$

Finally, the basic LMIs

$$\boldsymbol{\psi}_i + (\boldsymbol{P}^{(\mathrm{pLPV})})^{\mathrm{T}} \boldsymbol{\Omega}_i \boldsymbol{Q}^{(\mathrm{pLPV})} + (\boldsymbol{Q}^{(\mathrm{pLPV})})^{\mathrm{T}} \boldsymbol{\Omega}_i \boldsymbol{P}^{(\mathrm{pLPV})} < 0 \tag{60}$$

are solved for $\boldsymbol{\Omega}_i$ for every i.

The state-spaces matrices of the controllers for each vertex can be extracted from

$$\boldsymbol{\Omega}_i = \begin{bmatrix} \boldsymbol{A}_{K_i} & \boldsymbol{B}_{K_i} \\ \boldsymbol{C}_{K_i} & D_{K_i} \end{bmatrix}. \tag{61}$$

The implemented controller is interpolated using the coordinate vector $\boldsymbol{\lambda}$ in

$$\boldsymbol{\Omega}^{(\mathrm{pLPV})} = \Sigma_{i=1}^{m} \lambda_i \boldsymbol{\Omega}_i. \tag{62}$$

5.2. Controller synthesis and implementation for LPV-LFT systems

In this section, the algorithm for the calculation of the H_∞-suboptimal gain-scheduling controller from [1] is explained in detail.

From the state-space representation of the generalized plant the outer factors for the LMIs that have to be solved in the design can be calculated as

$$\boldsymbol{N}_{\boldsymbol{R}} = \mathrm{null} \begin{bmatrix} (\boldsymbol{B}_u^{(\mathrm{LFT})})^{\mathrm{T}} & \boldsymbol{D}_{\theta u}^{(\mathrm{LFT})} & (\boldsymbol{D}_{qu}^{(\mathrm{LFT})})^{\mathrm{T}} & \mathbf{0} \end{bmatrix} \tag{63}$$

and

$$\boldsymbol{N_S} = \text{null}\begin{bmatrix} \boldsymbol{C}_y^{(\text{LFT})} & \boldsymbol{D}_{y\theta} & \boldsymbol{D}_{yw}^{(\text{LFT})} & \boldsymbol{0} \end{bmatrix}. \tag{64}$$

With the outer factors, a first set of LMIs corresponding to the feasibility and optimality condition is given as

$$\boldsymbol{N_R}^{\mathrm{T}} \begin{bmatrix} \boldsymbol{A}\boldsymbol{R}\boldsymbol{A}^{\mathrm{T}} - \boldsymbol{R} & \boldsymbol{A}\boldsymbol{R}\boldsymbol{C}_\theta^{\mathrm{T}} & \boldsymbol{A}\boldsymbol{R}(\boldsymbol{C}^{(\text{LFT})})_q^{\mathrm{T}} & \boldsymbol{B}_\theta & \boldsymbol{B}_w \\ \boldsymbol{C}_\theta\boldsymbol{R}\boldsymbol{A}^{\mathrm{T}} & -\gamma\boldsymbol{J}_3 + \boldsymbol{C}_\theta\boldsymbol{R}\boldsymbol{C}_\theta^{\mathrm{T}} & \boldsymbol{C}_\theta\boldsymbol{R}(\boldsymbol{C}^{(\text{LFT})})_q^{\mathrm{T}} & \boldsymbol{D}_{\theta\theta} & \boldsymbol{D}_{\theta w} \\ \boldsymbol{C}_q^{(\text{LFT})}\boldsymbol{R}\boldsymbol{A}^{\mathrm{T}} & \boldsymbol{C}_q^{(\text{LFT})}\boldsymbol{R}\boldsymbol{C}_\theta^{\mathrm{T}} & \boldsymbol{C}_q^{(\text{LFT})}\boldsymbol{R}(\boldsymbol{C}^{(\text{LFT})})_q^{\mathrm{T}} - \gamma\mathbf{I} & \boldsymbol{D}_{q\theta} & \boldsymbol{D}_{qw}^{(\text{LFT})} \\ \boldsymbol{B}_\theta^{\mathrm{T}} & \boldsymbol{D}_{\theta\theta}^{\mathrm{T}} & \boldsymbol{D}_{q\theta}^{\mathrm{T}} & -\gamma\boldsymbol{L}_3 & \boldsymbol{0} \\ (\boldsymbol{B}_w^{(\text{LFT})})^{\mathrm{T}} & \boldsymbol{D}_{\theta w}^{\mathrm{T}} & (\boldsymbol{D}_{qw}^{(\text{LFT})})^{\mathrm{T}} & \boldsymbol{0} & -\gamma \end{bmatrix} \boldsymbol{N_R} < 0, \tag{65}$$

$$\boldsymbol{N_S}^{\mathrm{T}} \begin{bmatrix} \boldsymbol{A}^{\mathrm{T}}\boldsymbol{S}\boldsymbol{A} - \boldsymbol{S} & \boldsymbol{A}^{\mathrm{T}}\boldsymbol{S}\boldsymbol{B}_\theta & \boldsymbol{A}^{\mathrm{T}}\boldsymbol{S}\boldsymbol{B}_w^{(\text{LFT})} & \boldsymbol{C}_\theta^{\mathrm{T}} & (\boldsymbol{C}_q^{(\text{LFT})})^{\mathrm{T}} \\ \boldsymbol{B}_\theta^{\mathrm{T}}\boldsymbol{S}\boldsymbol{A} & -\gamma\boldsymbol{L}_3 + \boldsymbol{B}_\theta^{\mathrm{T}}\boldsymbol{S}\boldsymbol{B}_\theta & \boldsymbol{B}_\theta^{\mathrm{T}}\boldsymbol{S}\boldsymbol{B}_w^{(\text{LFT})} & \boldsymbol{D}_{\theta\theta}^{\mathrm{T}} & \boldsymbol{D}_{q\theta}^{\mathrm{T}} \\ (\boldsymbol{B}_w^{(\text{LFT})})^{\mathrm{T}}\boldsymbol{S}\boldsymbol{A} & (\boldsymbol{B}_w^{(\text{LFT})})^{\mathrm{T}}\boldsymbol{S}\boldsymbol{B}_\theta & (\boldsymbol{B}_w^{(\text{LFT})})^{\mathrm{T}}\boldsymbol{S}(\boldsymbol{B}_w^{(\text{LFT})}) - \gamma & \boldsymbol{D}_{\theta w}^{\mathrm{T}} & (\boldsymbol{D}_{qw}^{(\text{LFT})})^{\mathrm{T}} \\ \boldsymbol{C}_\theta & \boldsymbol{D}_{\theta\theta} & \boldsymbol{D}_{\theta w} & -\gamma\boldsymbol{J}_3 & \boldsymbol{0} \\ \boldsymbol{C}_q^{(\text{LFT})} & \boldsymbol{D}_{q\theta} & \boldsymbol{D}_{qw}^{(\text{LFT})} & \boldsymbol{0} & -\gamma\mathbf{I} \end{bmatrix} \boldsymbol{N_S} < 0, \tag{66}$$

$$\begin{bmatrix} \boldsymbol{R} & \mathbf{I} \\ \mathbf{I} & \boldsymbol{S} \end{bmatrix} \geq 0, \tag{67}$$

$$\begin{bmatrix} \boldsymbol{L}_3 & \mathbf{I} \\ \mathbf{I} & \boldsymbol{J}_3 \end{bmatrix} \geq 0. \tag{68}$$

The scalar γ is an upper bound of the maximum singular value, which is given as a constraint. This set of LMIs is solved for $\boldsymbol{R}$, $\boldsymbol{S}$, $\boldsymbol{J}_3$ and $\boldsymbol{L}_3$.

The matrices $\boldsymbol{L}_1$ and $\boldsymbol{L}_2$ are calculated through

$$\boldsymbol{L}_3 - \boldsymbol{J}_3^{-1} = \boldsymbol{L}_2^{\mathrm{T}}\boldsymbol{L}_1^{-1}\boldsymbol{L}_2, \tag{69}$$

and the matrix $\boldsymbol{X}^{(\text{LFT})}$ is computed as

$$\boldsymbol{X}^{(\text{LFT})} = \begin{bmatrix} \boldsymbol{S} & \mathbf{I} \\ \boldsymbol{N}^{\mathrm{T}} & \boldsymbol{0} \end{bmatrix} \begin{bmatrix} \mathbf{I} & \boldsymbol{R} \\ \boldsymbol{0} & \boldsymbol{M}^{\mathrm{T}} \end{bmatrix}, \tag{70}$$

with $\boldsymbol{M}$ and $\boldsymbol{N}$ satisfying

$$\boldsymbol{M}\boldsymbol{N}^{\mathrm{T}} = \mathbf{I} - \boldsymbol{R}\boldsymbol{S}. \tag{71}$$

Then, the basic LMI

$$\boldsymbol{\psi} + (\boldsymbol{Q}^{(\text{LFT})})^{\mathrm{T}}(\boldsymbol{\Omega}^{(\text{LFT})})^{\mathrm{T}}\boldsymbol{P}^{(\text{LFT})} + (\boldsymbol{P}^{(\text{LFT})})^{\mathrm{T}}\boldsymbol{\Omega}^{(\text{LFT})}\boldsymbol{Q}^{(\text{LFT})} < 0, \tag{72}$$

where

$$\boldsymbol{\psi} = \begin{bmatrix} -\boldsymbol{X}^{-1} & \boldsymbol{A}_0 & \boldsymbol{B}_0 & \boldsymbol{0} \\ \boldsymbol{A}_0^{\mathrm{T}} & -\boldsymbol{X} & \boldsymbol{0} & \boldsymbol{C}_0^{\mathrm{T}} \\ \boldsymbol{B}_0^{\mathrm{T}} & \boldsymbol{0} & -\gamma\boldsymbol{L}_0 & \boldsymbol{D}_0^{\mathrm{T}} \\ \boldsymbol{0} & \boldsymbol{C}_0 & \boldsymbol{D}_0 & -\gamma\boldsymbol{J}_0 \end{bmatrix}, \tag{73}$$

$$\boldsymbol{P}^{(\text{LFT})} = \begin{bmatrix} \check{\boldsymbol{B}}^{\mathrm{T}} & \boldsymbol{0} & \boldsymbol{0} & \check{\boldsymbol{D}}_{12}^{\mathrm{T}} \end{bmatrix}, \tag{74}$$

$$\boldsymbol{Q}^{(\mathrm{LFT})} = \begin{bmatrix} \mathbf{0} & \tilde{\boldsymbol{C}} & \tilde{\boldsymbol{D}}_{21} & \mathbf{0} \end{bmatrix}, \tag{75}$$

$$\boldsymbol{A}_0 = \begin{bmatrix} \boldsymbol{A} & \mathbf{0} \\ \mathbf{0} & \mathbf{0} \end{bmatrix}, \boldsymbol{B}_0 = \begin{bmatrix} \mathbf{0} & \boldsymbol{B}_\theta & \boldsymbol{B}_w^{(\mathrm{LFT})} \\ \mathbf{0} & \mathbf{0} & \mathbf{0} \end{bmatrix}, \tilde{\boldsymbol{B}} = \begin{bmatrix} \mathbf{0} & \boldsymbol{B}_u^{(\mathrm{LFT})} & \mathbf{0} \\ \mathbf{I} & \mathbf{0} & \mathbf{0} \end{bmatrix}, \tag{76}$$

$$\boldsymbol{C}_0 = \begin{bmatrix} \mathbf{0} & \mathbf{0} \\ \boldsymbol{C}_\theta & \mathbf{0} \\ \boldsymbol{C}_q^{(\mathrm{LFT})} & \mathbf{0} \end{bmatrix}, \tilde{\boldsymbol{C}} = \begin{bmatrix} \mathbf{0} & \mathbf{I} \\ \boldsymbol{C}_y^{(\mathrm{LFT})} & \mathbf{0} \\ \mathbf{0} & \mathbf{0} \end{bmatrix}, \boldsymbol{D}_0 = \begin{bmatrix} \mathbf{0} & \mathbf{0} & \mathbf{0} \\ \mathbf{0} & \boldsymbol{D}_{\theta\theta} & \boldsymbol{D}_{\theta w} \\ \mathbf{0} & \boldsymbol{D}_{q\theta} & \boldsymbol{D}_{qw}^{(\mathrm{LFT})} \end{bmatrix}, \tag{77}$$

$$\tilde{\boldsymbol{D}}_{12} = \begin{bmatrix} \mathbf{0} & \mathbf{0} & \mathbf{I} \\ \mathbf{0} & \boldsymbol{D}_{\theta u} & \mathbf{0} \\ \mathbf{0} & \boldsymbol{D}_{qu}^{(\mathrm{LFT})} & \mathbf{0} \end{bmatrix}, \tilde{\boldsymbol{D}}_{21} = \begin{bmatrix} \mathbf{0} & \mathbf{0} & \mathbf{0} \\ \mathbf{0} & \boldsymbol{D}_{y\theta} & D_{yw}^{(\mathrm{LFT})} \\ \mathbf{I} & \mathbf{0} & \mathbf{0} \end{bmatrix}, \tag{78}$$

and

$$\boldsymbol{L} = \begin{bmatrix} \boldsymbol{L}_1 & \boldsymbol{L}_2 \\ \boldsymbol{L}_2^{\mathrm{T}} & \boldsymbol{L}_3 \end{bmatrix}, \boldsymbol{L}_0 = \begin{bmatrix} \boldsymbol{L} & \mathbf{0} \\ \mathbf{0} & 1 \end{bmatrix}, \boldsymbol{J} = \boldsymbol{L}^{-1}, \boldsymbol{J}_0 = \begin{bmatrix} \boldsymbol{J} & \mathbf{0} \\ \mathbf{0} & \mathbf{I} \end{bmatrix}, \tag{79}$$

is solved for the controller matrix $\boldsymbol{\Omega}^{(\mathrm{LFT})}$. In the last step, the state-space matrices of the controller are extracted from

$$\boldsymbol{\Omega}^{(\mathrm{LFT})} = \begin{bmatrix} \boldsymbol{A}_K^{(\mathrm{LFT})} & \boldsymbol{B}_K^{(\mathrm{LFT})} \\ \boldsymbol{C}_K^{(\mathrm{LFT})} & \boldsymbol{D}_K^{(\mathrm{LFT})} \end{bmatrix}. \tag{80}$$

6. Experimental results

The gain-scheduled output-feedback controllers obtained through the design procedures presented in this chapter are validated with experimental results. Both controllers have been tested on the ANC and AVC systems. Results are presented for the pLPV gain-scheduled controller on the ANC system in Sec. 6.1 and for the LPV-LFT controller on the AVC test bed in Sec. 6.2. Identical hardware setup and sampling frequency as in the previous chapter are used.

6.1. Experimental results for the pLPV gain-scheduled controller

The pLPV gain-scheduled controller is validated with experimental results on the ANC headset. The controller is designed to reject a disturbance signal which contains four harmonically related sine signals with fundamental frequency between 80 and 90 Hz. The controller obtained is of 21st order.

Amplitude frequency responses and pressure measured when the fundamental frequency rises suddenly from 80 to 90 Hz are shown in Figs. 6 and 7. An excellent disturbance rejection is achieved even for unrealistically fast variations of the disturbance frequencies. In Fig. 8, results for time-varying frequencies are shown. The performance for fast variations of the fundamental frequency is further studied in Fig. 9. As in the previous chapter, with fast changes of the fundamental frequency the disturbance attenuation performance decreases but the system remains stable.

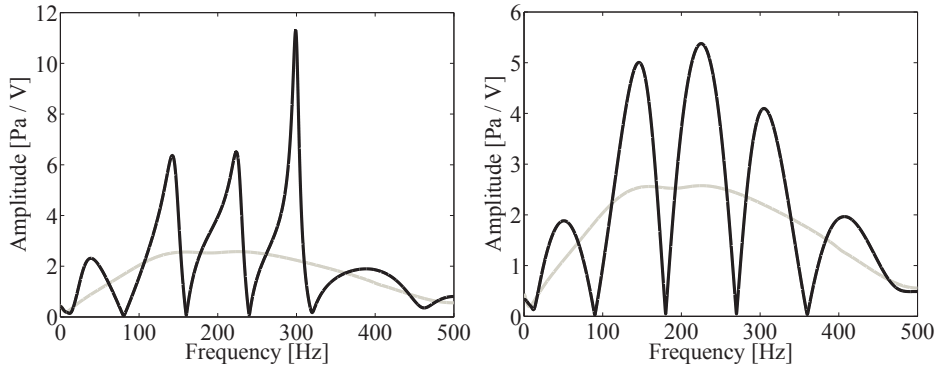

Figure 6. Open-loop (gray) and closed-loop (black) amplitude frequency responses for fixed disturbance frequencies of 80, 160, 240 and 320 Hz (left) and of 90, 180, 270 and 360 Hz (right)

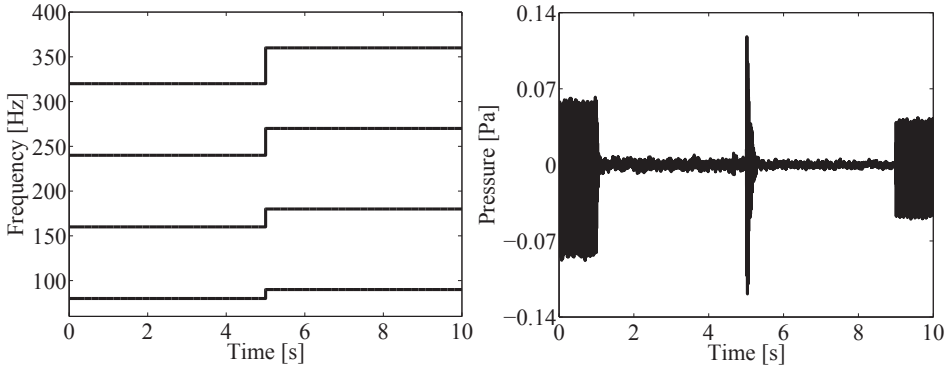

Figure 7. Results for a disturbance with time-varying frequencies. Variation of the frequencies (left) and measured sound pressure (right). The control sequence is off/on/off

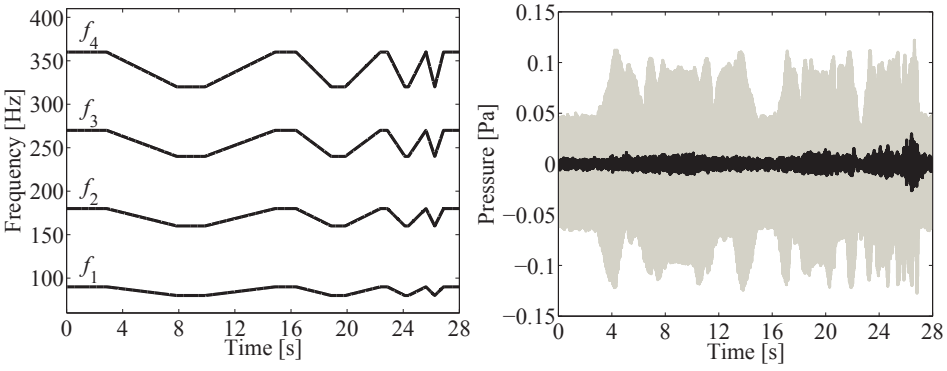

Figure 8. Results for a disturbance with time-varying frequencies. Variation of the frequencies (left) and measured sound pressure (right) in open loop (gray) and closed loop (black)

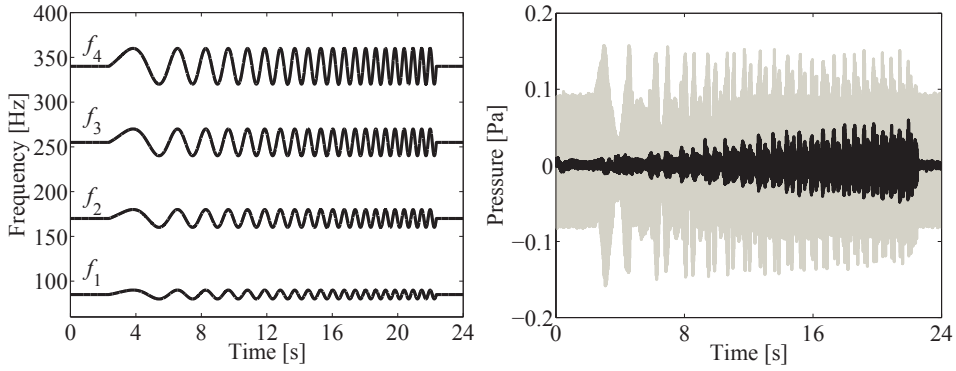

Figure 9. Results for a disturbance with time-varying frequencies. Variation of the frequencies (left) and measured sound pressure (right) in open loop (gray) and closed loop (black)

6.2. Experimental results for the LFT gain-scheduled controller

The AVC test bed is used to test the LFT gain-scheduled controller experimentally. The controller is designed to reject a disturbance with eight harmonic components which are selected to be uniformly distributed from 80 to 380 Hz in intervals of 20 Hz. The resulting controller is of 27th order.

Amplitude frequency responses are shown in Fig. 10 and results for an experiment where the frequencies change drastically as a step function in Fig. 11. Results from experiments with time-varying frequencies are shown in Figs. 12 and 13. Excellent disturbance rejection is achieved.

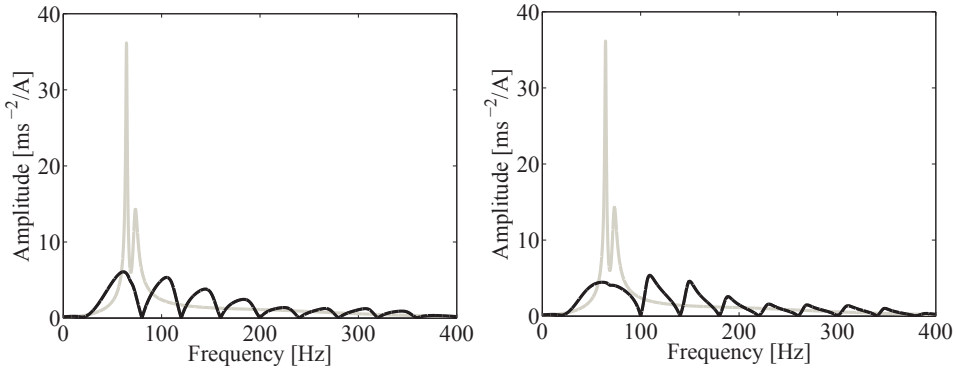

Figure 10. Open-loop (gray) and closed-loop (black) amplitude frequency responses for fixed disturbance frequencies of 80, 120, 160, 200, 240, 280, 320 and 360 Hz (left) and 100, 140, 180, 220, 260, 300, 340 and 380 Hz (right)

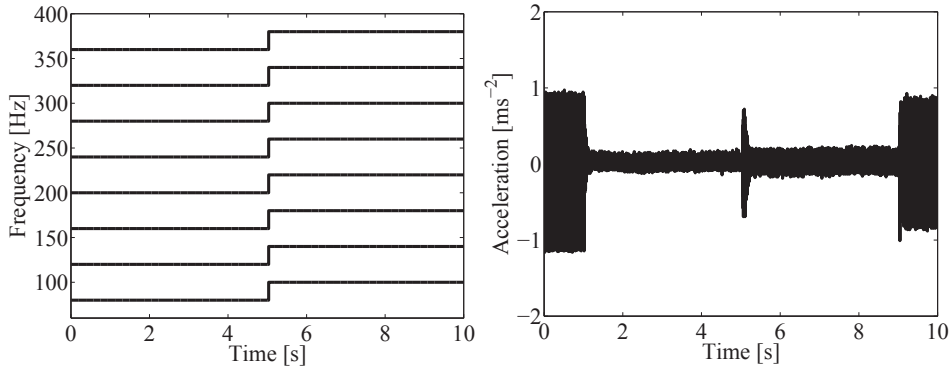

Figure 11. Results for a disturbance with time-varying frequencies. Variation of the frequencies (left) and measured acceleration (right). The control sequence is off/on/off

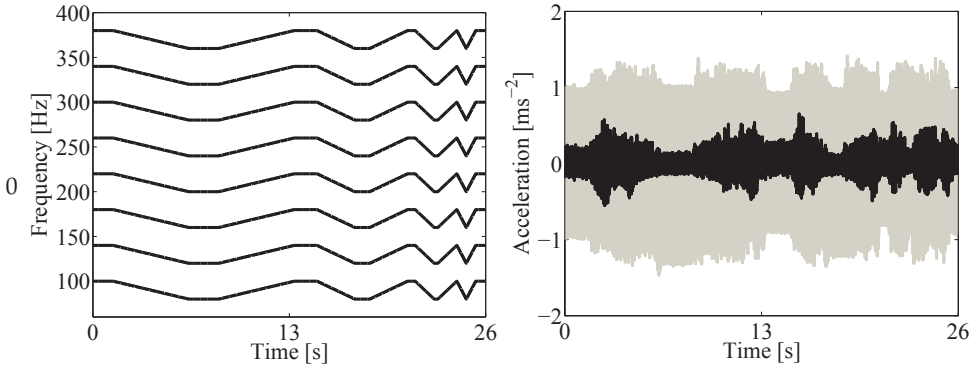

Figure 12. Results for a disturbance with time-varying frequencies. Variation of the frequencies (left) and measured acceleration (right) in open loop (gray) and closed loop (black)

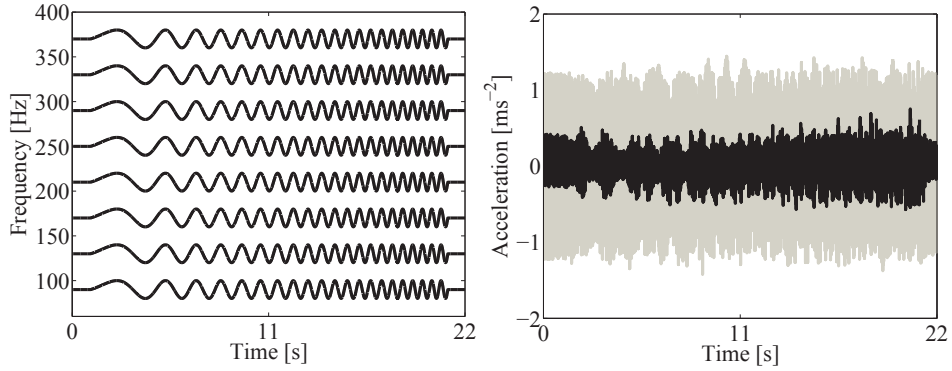

Figure 13. Results for a disturbance with time-varying frequencies. Variation of the frequencies (left) and measured acceleration (right) in open loop (gray) and closed loop (black)

7. Discussion and conclusion

Two discrete-time control design methods have been presented in this chapter for the rejection of time-varying frequencies. The output-feedback controllers are obtained through pLPV and LPV-LFT gain-scheduling techniques. The controllers obtained are validated experimentally on an ANC and AVC system. The experimental results show an excellent disturbance rejection even for the case of eight frequency components of the disturbance.

The control design guarantees stability even for arbitrarily fast changes of the disturbance frequencies. This is an advantage over heuristic interpolation methods or adaptive filtering, for which none or only "approximate stability results" are available [10].

To the best of the authors' knowledge, industrial applications of LPV controllers are rather limited. The results of this chapter show that the implementation of even high-order LPV controllers can be quite straightforward.

Nomenclature

Acronyms

ANC	Active noise control.
AVC	Active vibration control.
LFT	Linear fractional transformation.
LMI	Linear matrix inequality.
LPV	Linear parameter varying.
LTI	Linear time invariant.
pLPV	Polytopic linear parameter varying.

Variables

(in order of appearance)

$\boldsymbol{G}$	Generalized plant.
$\boldsymbol{K}$	Controller.
$\boldsymbol{u}, \boldsymbol{y}$	Control input, output signal.
$\boldsymbol{w}, \boldsymbol{q}$	Performance input, performance output.
$\sigma_{\max}$	Maximum singular value.
G_{qw}	Transfer path between performance input and performance output.
$\boldsymbol{A}(\boldsymbol{\theta}), \boldsymbol{B}, \boldsymbol{C}, \boldsymbol{D}$	State-space matrices of a pLPV system.
$\boldsymbol{x}_k, \boldsymbol{y}_k, \boldsymbol{u}_k$	State vector, output and input.

$\boldsymbol{\mathcal{A}}_i$	Constant matrices of the polytopic representation of $\boldsymbol{A}(\boldsymbol{\theta})$.
$\boldsymbol{\theta}$	Parameter vector.
θ_i	The i-th element of the parameter vector.
$\boldsymbol{\Theta}$	Parameter polytope.
$\boldsymbol{v}_j$	Vertices of the polytope.
M	Number of vertices of the polytope.
N	Number of parameters.
$\boldsymbol{\lambda}$	Coordinate vector.
λ_j	The j-th element of the coordinate vector.
$\boldsymbol{A}_{\mathrm{v},j}, \boldsymbol{A}(v_j)$	System matrix for the j-th vertex.
$\overline{\boldsymbol{\theta}}$	Parametric uncertainty block.
$\boldsymbol{w}_\theta, \boldsymbol{q}_\theta$	Output and input of the parameter block for the plant in LFT form.
$\tilde{\boldsymbol{w}}_\theta, \tilde{\boldsymbol{q}}_\theta$	Output and input of the parameter block for the controller in LFT form.
n_d	Number of frequencies of the disturbance.
$\boldsymbol{A}_\mathrm{d}^{(2n_\mathrm{d}\times 2n_\mathrm{d})}$, $\boldsymbol{B}_\mathrm{d}^{(2n_\mathrm{d}\times 1)}$, $\boldsymbol{C}_\mathrm{d}^{(1\times 2n_\mathrm{d})}$	State-space matrices of the disturbance model for fixed frequencies.
$\boldsymbol{A}_{\mathrm{d},i}, \boldsymbol{B}_{\mathrm{d},i}, \boldsymbol{C}_{\mathrm{d},i}$	Block matrices of $\boldsymbol{A}_\mathrm{d}$, $\boldsymbol{B}_\mathrm{d}$ and $\boldsymbol{C}_\mathrm{d}$.
a_i	Scalar parameter for the disturbance model.
T, f_i	Sampling time and the i-th frequency.
$\boldsymbol{A}_\mathrm{d}(\boldsymbol{\theta})^{(2n_\mathrm{d}\times 2n_\mathrm{d})}$, $\boldsymbol{B}_\mathrm{d}^{(2n_\mathrm{d}\times 1)}$, $\boldsymbol{C}_\mathrm{d}^{(1\times 2n_\mathrm{d})}$	State-space matrices of the pLPV disturbance model.
$\boldsymbol{\mathcal{A}}_{\mathrm{d},i}$	Constant matrices of the polytopic representation of $\boldsymbol{A}_\mathrm{d}(\boldsymbol{\theta})$.
n_p	Order of the plant.
G_p	System representation of the plant.
$\boldsymbol{A}_\mathrm{p}^{(n_\mathrm{p}\times n_\mathrm{p})}$, $\boldsymbol{B}_\mathrm{p}^{(n_\mathrm{p}\times 1)}$, $\boldsymbol{C}_\mathrm{p}^{(1\times n_\mathrm{p})}, D_\mathrm{p}^{(1\times 1)}$	State-space matrices of the plant.
n_{W_y}	Order of the weighting function for y.

W_y, W_u	System representations of the weighting functions.
$\boldsymbol{A}_{W_y}^{(n_{W_y}\times n_{W_y})}, \boldsymbol{B}_{W_y}^{(n_{W_y}\times 1)}, \boldsymbol{C}_{W_y}^{(1\times n_{W_y})}, D_{W_y}^{(1\times 1)}$	State-space matrices of the weighting function for y.
n_{W_u}	Order of the weighting function for u.
$\boldsymbol{A}_{W_u}^{(n_{W_u}\times n_{W_u})}, \boldsymbol{B}_{W_u}^{(n_{W_u}\times 1)}, \boldsymbol{C}_{W_u}^{(1\times n_{W_u})}, D_{W_u}^{(1\times 1)}$	State-space matrices of the weighting function for u.
$\boldsymbol{x}_{\mathrm{p},k}, \boldsymbol{x}_{\mathrm{d},k}, \boldsymbol{x}_{W_y,k}, \boldsymbol{x}_{W_u,k}$	State vectors of plant, disturbance and weighting functions.
$\boldsymbol{A}_i(\boldsymbol{\theta}), \boldsymbol{B}_w^{(\mathrm{pLPV})}, \boldsymbol{B}_u^{(\mathrm{pLPV})}, \boldsymbol{C}_q^{(\mathrm{pLPV})}, \boldsymbol{D}_{qw}^{(\mathrm{pLPV})}, \boldsymbol{D}_{qu}^{(\mathrm{pLPV})}, \boldsymbol{C}_y^{(\mathrm{pLPV})}, D_{yw}^{(\mathrm{pLPV})}, D_{qw}^{(\mathrm{pLPV})}$	State-space matrices of the pLPV generalized plant.
$\mathbf{0}$	Zero matrix.
$\boldsymbol{A}_{\mathrm{d}}, \boldsymbol{B}_{\mathrm{d},\theta}, \boldsymbol{B}_{\mathrm{d},w}, \boldsymbol{C}_{\mathrm{d},\theta}, \boldsymbol{C}_{\mathrm{d},y}$	State-space matrices of the LFT disturbance model.
$w_{\mathrm{d}}, y_{\mathrm{d}}$	Input and output of the disturbance model.
$u_{\mathrm{p}}, y_{\mathrm{p}}$	Input and output of the plant.
$\overline{a}_i, p_i$	Scalar parameters for the disturbance model.
$\boldsymbol{A}, \boldsymbol{B}_\theta, \boldsymbol{B}_w^{(\mathrm{LFT})}, \boldsymbol{B}_u^{(\mathrm{LFT})}, \boldsymbol{C}_\theta, \boldsymbol{D}_{\theta\theta}, \boldsymbol{D}_{\theta w}, \boldsymbol{D}_{\theta u}, \boldsymbol{C}_q^{(\mathrm{LFT})}, \boldsymbol{D}_{q\theta}, \boldsymbol{D}_{qw}^{(\mathrm{LFT})}, \boldsymbol{D}_{qu}^{(\mathrm{LFT})}, \boldsymbol{C}_y^{(\mathrm{LFT})}, \boldsymbol{D}_{y\theta}, \boldsymbol{D}_{yw}^{(\mathrm{LFT})}, \boldsymbol{D}_{yu}^{(\mathrm{LFT})}$	State-space matrices of the LFT generalized plant.
$\boldsymbol{N}_{\boldsymbol{X}}^{((n+3)\times(n+2))}, \boldsymbol{N}_{\boldsymbol{Y}}^{((n+3)\times(n+2))}$	Outer factors to build the LMIs.
$\boldsymbol{X}_1^{(n\times n)}, \boldsymbol{Y}_1^{(n\times n)}$	Solutions of the first set of LMIs.
$\mathbf{I}$	Identitiy matrix.
$n = n_{\mathrm{p}} + 2n_{\mathrm{d}} + n_{W_y} + n_{W_u}$	Order of matrices $\boldsymbol{X}_1$ and $\boldsymbol{Y}_1$.
$\boldsymbol{\psi}_i^{(4n+3)\times(4n+3)}$	Matrix to build the basic LMI.
$\boldsymbol{X}^{(2n\times 2n)}, \overline{\boldsymbol{A}}_i^{(2n\times 2n)}, \overline{\boldsymbol{B}}^{(2n\times 1)}, \overline{\boldsymbol{C}}^{(2\times 2n)}$	Matrices to build matrix $\boldsymbol{\psi}_i$.
$\boldsymbol{P}^{((n+1)\times(4n+3))}, \boldsymbol{Q}^{((n+1)\times(4n+3))}$	Matrices to build the basic LMI.

$\underline{\boldsymbol{B}}^{(2n\times(n+1))}, \underline{\boldsymbol{C}}^{((n+1)\times 2n)}$, $\underline{\boldsymbol{D}}_{qu}^{(2\times(n+1))}, \underline{\boldsymbol{D}}_{yw}^{((n+1)\times 1)}$	Matrices to obtain $\boldsymbol{P}^{(\mathrm{pLPV})}$ and $\boldsymbol{Q}^{(\mathrm{pLPV})}$.
$\boldsymbol{\Omega}_i^{((n+1)\times(n+1))}$	Solution of the basic LMI for the i-th vertex.
$\boldsymbol{A}_{K_i}^{(n\times n)}, \boldsymbol{B}_{K_i}^{(n\times 1)}$, $\boldsymbol{C}_{K_i}^{(1\times n)}, D_{K_i}^{(1\times 1)}$	State-space matrices of the controller for the i-th vertex.
$\boldsymbol{N}_{\boldsymbol{R}}^{((n+2n_\mathrm{d}+3)\times(n+2n_\mathrm{d}+2))}$, $\boldsymbol{N}_{\boldsymbol{S}}^{((n+2n_\mathrm{d}+3)\times(n+2n_\mathrm{d}+2))}$	Outer factors to build the LMIs.
$\boldsymbol{R}^{(n\times n)}, \boldsymbol{S}^{(n\times n)}$, $\boldsymbol{J}_3^{(n_\mathrm{d}\times n_\mathrm{d})}, \boldsymbol{L}_3^{(n_\mathrm{d}\times n_\mathrm{d})}$	Solutions of the first set of LMIs.
γ	Upper bound of the maximum singular value.
$\boldsymbol{M}^{(n\times n)}, \boldsymbol{N}^{(n\times n)}$	Matrices calculated from $\boldsymbol{R}$ and $\boldsymbol{S}$.
$\boldsymbol{L}_1^{(n_\mathrm{d}\times n_\mathrm{d})}, \boldsymbol{L}_2^{(n_\mathrm{d}\times n_\mathrm{d})}$	Matrices to build $\boldsymbol{L}$.
$\boldsymbol{\psi}^{((4n+4n_\mathrm{d}+3)\times(4n+4n_\mathrm{d}+3))}$	Matrix to build the basic LMI.
$\boldsymbol{X}^{(2n\times 2n)}, \boldsymbol{A}_0^{(2n\times 2n)}$, $\boldsymbol{B}_0^{(2n\times(2n_\mathrm{d}+1))}, \boldsymbol{C}_0^{((2n_\mathrm{d}+2)\times 2n)}$ $\boldsymbol{D}_0^{((2n_\mathrm{d}+2)\times(2n_\mathrm{d}+1))}, \boldsymbol{J}_0^{((2n_\mathrm{d}+2)\times(2n_\mathrm{d}+2))}$, $\boldsymbol{L}_0^{((2n_\mathrm{d}+1)\times(2n_\mathrm{d}+1))}, \boldsymbol{J}^{(2n_\mathrm{d}\times 2n_\mathrm{d})}$, $\boldsymbol{L}^{(2n_\mathrm{d}\times 2n_\mathrm{d})}$	Matrices needed to build ψ.
$\boldsymbol{P}^{((n+n_\mathrm{d}+1)\times(4n+4n_\mathrm{d}+3))}$, $\boldsymbol{Q}^{((n+n_\mathrm{d}+1)\times(4n+4n_\mathrm{d}+3))}$	Matrices to build the basic LMI.
$\tilde{\boldsymbol{B}}^{(2n\times(n+n_\mathrm{d}+1))}, \tilde{\boldsymbol{C}}^{((n+n_\mathrm{d}+1)\times 2n)}$, $\tilde{\boldsymbol{D}}_{12}^{((2n_\mathrm{d}+2)\times(n+n_\mathrm{d}+1))}$, $\tilde{\boldsymbol{D}}_{21}^{((n+n_\mathrm{d}+1)\times(2n_\mathrm{d}+1))}$	Matrices to obtain $\boldsymbol{P}^{(\mathrm{LFT})}$ and $\boldsymbol{Q}^{(\mathrm{LFT})}$.
$\boldsymbol{\Omega}^{((n+n_\mathrm{d}+1)\times(n+n_\mathrm{d}+1))}$	Controller matrix.
$\boldsymbol{A}_K^{(n\times n)}, \boldsymbol{B}_K^{(n\times(n_\mathrm{d}+1))}$, $\boldsymbol{C}_K^{((n_\mathrm{d}+1)\times n)}, \boldsymbol{D}_K^{((n_\mathrm{d}+1)\times(n_\mathrm{d}+1))}$	State-space matrices of the controller.

Author details

Pablo Ballesteros, Xinyu Shu, Wiebke Heins and Christian Bohn
Institute of Electrical Information Technology, Clausthal University of Technology, Clausthal-Zellerfeld, Germany

8. References

[1] Apkarian, P. and P. Gahinet. 1995. A convex charachterization of gain-scheduled H_∞ controllers. *IEEE Transactions on Automatic Control* 40:853-64.

[2] Ballesteros, P. and C. Bohn. 2011a. A frequency-tunable LPV controller for narrowband active noise and vibration control. *Proceedings of the American Control Conference*. San Francisco, June 2011. 1340-45.

[3] Ballesteros, P. and C. Bohn. 2011b. Disturbance rejection through LPV gain-scheduling control with application to active noise cancellation. *Proceedings of the IFAC World Congress*. Milan, August 2011. 7897-902.

[4] Balini, H. M. N. K., C. W. Scherer and J. Witte. 2011. Performance enhancement for AMB systems using unstable H_∞ controllers. *IEEE Transactions on Control Systems Technology* 19:1479-92.

[5] Bohn, C., A. Cortabarria, V. Härtel and K. Kowalczyk. 2003. Disturbance-observer-based active control of engine-induced vibrations in automotive vehicles. *Proceedings of the SPIE's 10th Annual International Symposium on Smart Structures and Materials*. San Diego, March 2003. Paper No. 5049-68.

[6] Bohn, C., A. Cortabarria, V. Härtel and K. Kowalczyk. 2004. Active control of engine-induced vibrations in automotive vehicles using disturbance observer gain scheduling. *Control Engineering Practice* 12:1029-39.

[7] Darengosse, C. and P. Chevrel. 2000. Linear parameter-varying controller design for active power filters. *Proceedings of the IFAC Control Systems Design*. Bratislava, June 2000. 65-70.

[8] Du, H. and X. Shi. 2002. Gain-scheduled control for use in vibration suppression of system with harmonic excitation. *Proceedings of the American Control Conference*. Anchorage, May 2002. 4668-69.

[9] Du, H., L. Zhang and X. Shi. 2003. LPV technique for the rejection of sinusoidal disturbance with time-varying frequency. *IEE Proceedings on Control Theory and Applications* 150:132-38.

[10] Feintuch, P. L., N. J. Bershad and A. K. Lo. 1993. A frequency-domain model for filtered LMS algorithms - Stability analysis, design, and elimination of the training mode. *IEEE Transactions on Signal Processing* 41:1518-31.

[11] Gahinet, P. and P. Apkarian. 1994. A linear matrix inequality approach to H_∞ control. *International Journal of Robust and Nonlinear Control* 4:421-48.

[12] Heins, W., P. Ballesteros and C. Bohn. 2011. Gain-scheduled state-feedback control for active cancellation of multisine disturbances with time-varying frequencies. Presented at the *10th MARDiH Conference on Active Noise and Vibration Control Methods*. Krakow-Wojanow, Poland, June 2011.

[13] Heins, W., P. Ballesteros and C. Bohn. 2012. Experimental evaluation of an LPV-gain-scheduled observer for rejecting multisine disturbances with time-varying frequencies. *Proceedings of the American Control Conference*. Montreal, June 2012. Accepted for publication.

[14] Kinney, C. E. and R. A. de Callafon. 2006a. Scheduling control for periodic disturbance attenuation. *Proceedings of the American Control Conference*. Minneapolis, June 2006. 4788-93.

[15] Kinney, C. E. and R. A. de Callafon. 2006b. An adaptive internal model-based controller for periodic disturbance rejection. *Proceedings of the 14th IFAC Symposium on System Identification*. Newcastle, Australia, March 2006. 273-78.

[16] Kinney, C. E. and R. A. de Callafon. 2007. A comparison of fixed point designs and time-varying observers for scheduling repetitive controllers. *Proceedings of the 46th IEEE Conference on Decision and Control*. New Orleans, December 2007. 2844-49.
[17] Köroğlu, H. and C. W. Scherer. 2008. LPV control for robust attenuation of non-stationary sinusoidal disturbances with measurable frequencies. *Proceedings of the 17th IFAC World Congress*. Korea, July 2008. 4928-33.
[18] Shu, X., P. Ballesteros and C. Bohn. 2011. Active vibration control for harmonic disturbances with time-varying frequencies through LPV gain scheduling. *Proceedings of the 23rd Chinese Control and Decision Conference*. Mianyang, China, May 2011. 728-33.
[19] Witte, J., H. M. N. K. Balini and C. W. Scherer. 2010. Experimental results with stable and unstable LPV controllers for active magnetic bearing systems. *Proceedings of the IEEE International Conference on Control Applications*. Yokohama, September 2010. 950-55.